Erzincan Üniversitesi
Fen Bilimleri Enstitüsü Dergisi
2022, 15(3), 931-941
ISSN: 1307-9085, e-ISSN: 2149-4584
Araştırma Makalesi

Erzincan University
Journal of Science and Technology
2022, 15(3), 931-941
DOI: 10.18185/erzifbed.1101771
Research Article

Structural, Surface and Optical Characterization of ZnO Thin Films Deposited by SILAR and Spin-Coating Methods

Melih Özden[1*] and Çağlar Duman[2]

[1*]Department of Electrical and Electronics Engineering, Erzincan Binali Yildirim University, Erzincan, Turkey
[2]Department of Electrical and Electronics Engineering, Erzurum Technical University, Erzurum, Turkey

Received:11/04/2022, **Revised:** 07/07/2022, **Accepted:** 17/07/2022, **Published:** 30/12/2022

Abstract

In this study, ZnO thin films were deposited on (1 1 1) oriented n-type and (1 0 0) oriented p-type Si substrates using SILAR and spin-coating methods, respectively. The XRD, SEM, and PL measurements of the samples were performed. The XRD results showed the presence of ZnO peaks. The SEM results showed that the surfaces were homogeneous in both methods. The PL results showed that the samples emitted light at different wavelengths. The PL results under different powers were interpreted from the samples, and it was determined that this sample reached a higher emission intensity with increasing excitation power.

Keywords: ZnO, SILAR, spin-coating, thin-film

SILAR ve Dönel Kaplama Yöntemleri Kullanılarak Büyütülen ZnO İnce Filmlerin Yapısal, Yüzeysel ve Optik Karakterizasyonu

Öz

Bu çalışmada, ZnO ince filmler sırasıyla (1 1 1) yönelimli n-tipi ve (1 0 0) yönelimli p-tipi Si altlıklar üzerine SILAR ve dönel kaplama (spin-coating) yöntemleri kullanılarak büyütülmüştür. Numunelerin XRD, SEM ve PL ölçümleri alınmıştır. XRD sonuçları, ZnO piklerinin varlığını göstermiştir. SEM sonuçları, yüzeylerin her iki yöntemde de homojen olduğunu göstermiştir. PL sonuçları, numunelerin farklı dalga boylarında ışık yaydığını göstermiştir. Örneklerden farklı güçler altında PL ölçümleri alınmış ve yorumlanmış ve bir örneğin artan uyartım gücü ile daha yüksek bir emisyon yoğunluğuna ulaştığı tespit edilmiştir.

Anahtar Kelimeler: ZnO, SILAR, dönel kaplama, ince film

*Corresponding Author: melih.ozden@erzincan.edu.tr
Melih Özden, https://orcid.org/0000-0002-6383-1464
Çağlar Duman, https://orcid.org/0000-0002-1845-8605

1. Introduction

Zinc oxide (ZnO) is a II-VI group compound and is a direct band semiconductor with high electrical conductivity and a bandgap of approximately 3.2-3.3 eV at room temperature [1-2]. One of the most significant advantages of ZnO is its high exciton binding energy (60 meV) [3]. In addition, it is a significant advantage that it is a material resistant to particle radiation damage [4]. Owing to these properties, ZnO has been used in solar cells, transparent conductive films, chemical sensors, varistors, LEDs, ultraviolet photodetectors, laser diodes, and gas sensors [5]. Various methods have been developed such as chemical vapor deposition (CVD) [6], RF magnetron sputtering [7], pulsed laser deposition [8], spray pyrolysis [9], metal oxide chemical vapor deposition (MOCVD) [10], electrochemical deposition [11], chemical bath deposition (CBD) [12], spin-coating [13-15] and successive ionic layer adsorption and reaction (SILAR) [16-18]. In this study, the spin-coating and SILAR methods were preferred for the deposition of ZnO thin films because these methods are simple, economical and more easily accessible than other methods. The remainder of this paper is organized as follows. In Section 2, the stages of the SILAR and spin-coating methods are described in detail. The structural, surface and optical characterizations and obtained results are discussed in Section 3. Finally, Section 4 concludes the paper.

2. Materials and Methods

2.1 Deposition of ZnO thin films

In this study, ZnO thin films were deposited using SILAR and spin-coating methods. In the SILAR method, 682 mg of zinc chloride ($ZnCl_2$) was added to 50 ml of deionized water to obtain a 0.1 M precursor cationic solution. The pH of the solution was adjusted to 10 by adding 6 ml ammonia (NH_3). The resulting solution was mixed for 5 min and then transferred to a beaker. A SILAR round was completed by keeping the substrates in a zinc chloride solution for 30 s, in air for 15 s and deionized water at 90°C for 10 s. This process was repeated for 100 cycles. Figure 1 shows a schematic of the SILAR cycle used to produce ZnO thin films. The chemical reactions that occur during the deposition of ZnO structures using the SILAR method are shown in Equation 1 to Equation 4 [17].

$$2ZnCl_2 + 4NH_3 \rightarrow 2Zn[(NH_3)_4]^{2+} + 2Cl^- \quad (1)$$

$$[Zn(NH_3)_4]^{2+} + H_2O \rightarrow Zn^{2+} + NH^{4+} + OH^- \quad (2)$$

$$Zn^{2+} + 2OH^- \rightarrow Zn(OH)_2 \quad (3)$$

$$Zn(OH)_2 \rightarrow ZnO(s) + H_2O \quad (4)$$

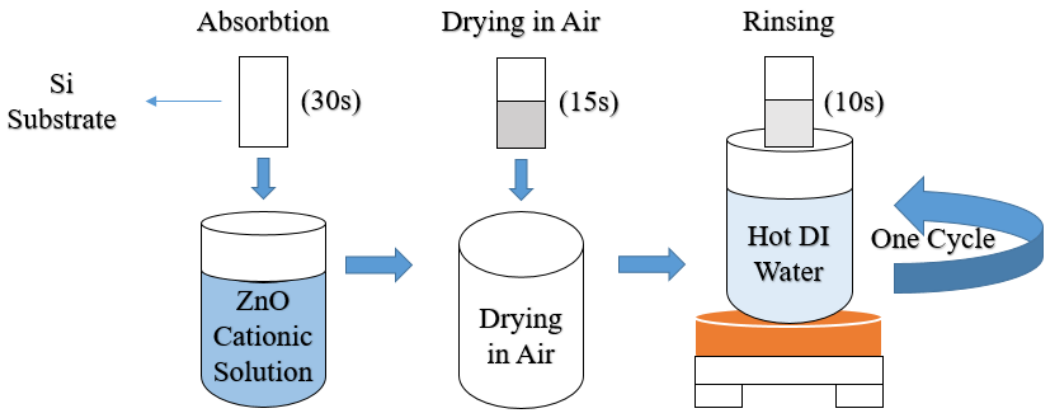

Figure 1. Schematic diagram of SILAR method.

The spin coating method starts with preparation of a 0.5M precursor solution. It was obtained by adding 5.48775g of zinc acetate dihydrate ($Zn(CH_3COO).2H_2O$) to 50ml of 2-methoxy ethanol ($C_3H_8O_2$). To obtain a 0.5M secondary solution, 1.512ml of monoethanolamine (C_2H_7NO) was mixed with 50ml of 2-methoxy ethanol ($C_3H_8O_2$). A homogeneous solution was formed by combining the two solutions in a beaker and mixing at 60°C for 2 h. The prepared solution was dripped onto a silicon substrate, and the substrate was spun at 3000 rpm for 30 s. The samples were then baked at 250°C for 10 min. These processes were repeated ten times, and the samples were annealed at 450°C for 30 min as the final step. Figure 2 shows the stages of the spin-coating method.

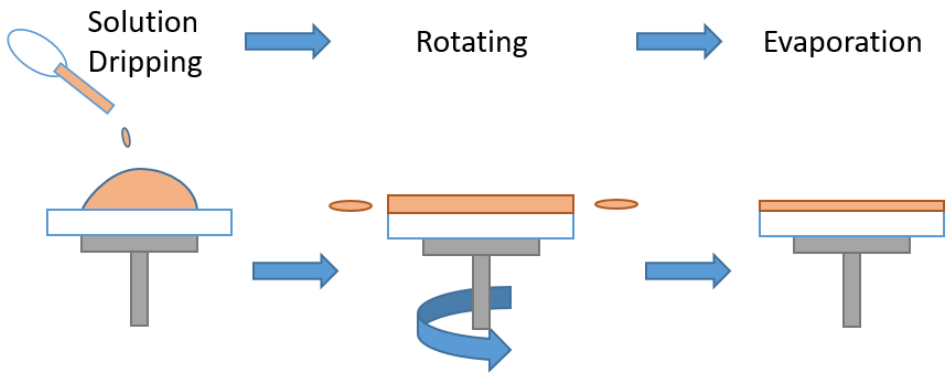

Figure 2. Schematic diagram of spin-coating method.

2.2 Characterization

A Laurell WS-650MZ-23NPPB0 spinner was used for film deposition via the spin-coating method. XRD, SEM, and PL were used for the structural, surface, and optical characterization of the ZnO thin films. For structural analysis, a GNR-Explorer X-ray diffractometer with Cu Kα (k=1.5405 Å) radiation for 2h at 10-60° was used. The surface morphology was studied using a Quanta FEG 250 SEM model. For the PL measurements, the 'MAPLE-II low-temperature macro photoluminescence system was used with laser excitation at 650 nm.

3. Results and discussion

Figure 3 shows the XRD measurement results of samples deposited on (1 1 1) oriented n-type and (1 0 0) oriented p-type Si by SILAR and spin-coating methods, respectively. When the figures are examined, it is understood that the marked peaks are compatible with the ZnO peaks reported in the literature [19], and the ZnO thin films grow in wurtzite structure.

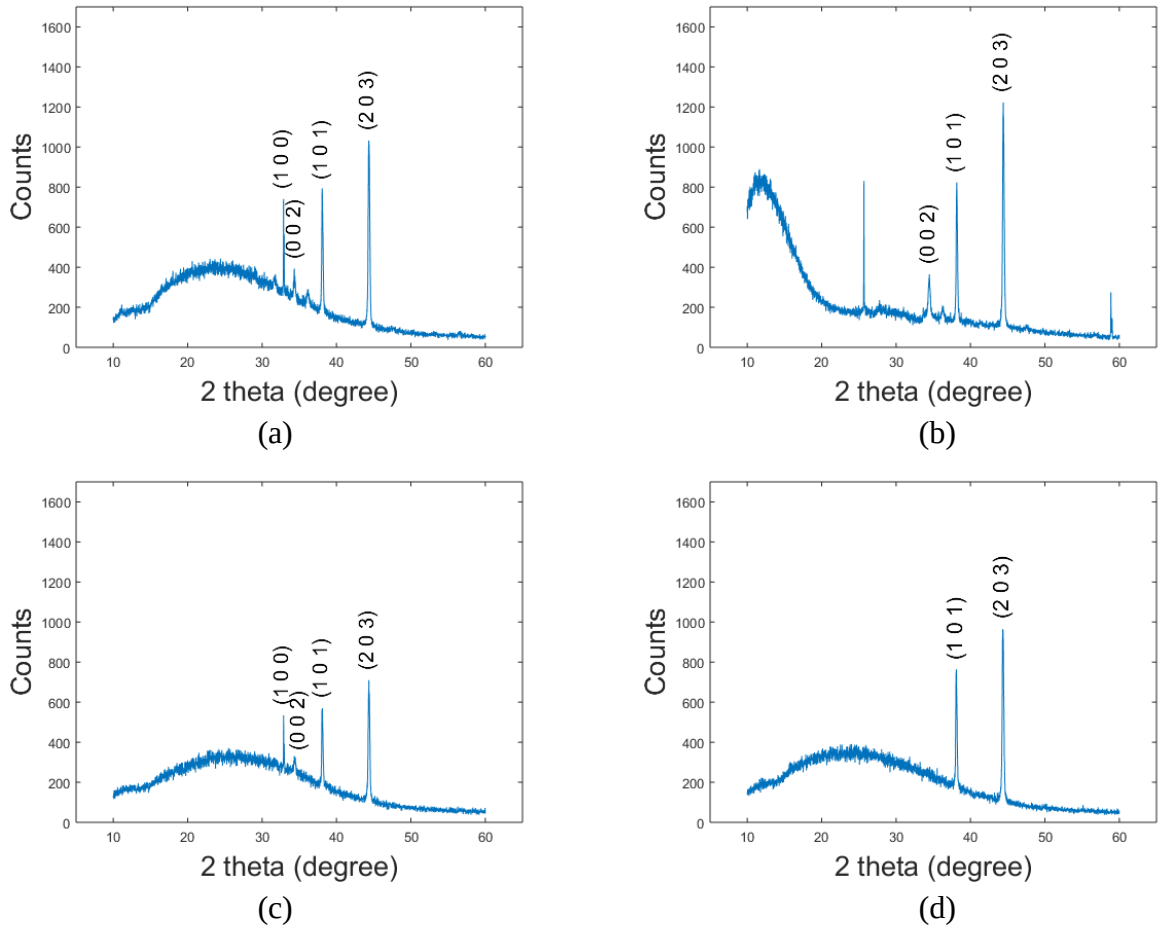

Figure 3. XRD measurement results of ZnO deposited by (a) SILAR method on n-type, (b) SILAR method on p-type Si, (c) spin coating method on n-type Si, (d) spin coating method on p-type Si.

Table 1 shows the micro strain values (ε), dislocation density (δ) datas, and crystal sizes (D) obtained from the XRD data.

Table 1. Crystal size calculation results from XRD results

	Miller indices	2θ (°)	FWHM (°)	ε (lin-m^4)x10^{-4}	δ (lin/m^2)*10^{14}	D (nm)
SILAR on n-type Si	100	32,88574	0,03440	1,439600	0,157860	251,69023
	002	34,34439	0,30026	12,51728	11,93454	28,946580
	101	38,10436	0,20674	8,526590	5,537790	42,494390
	203	44,36986	0,24618	9,946430	7,535630	36,428400
	002	34,45766	0,34117	14,21839	15,39879	25,483362

SILAR on p-type Si	101	38,16712	0,20866	8,604151	5,638995	42,111347
	203	44,42552	0,24520	9,904867	7,472793	36,581249
Spin coating on n-type Si	100	32,89336	0,03465	1,450030	0,160155	249,87918
	002	34,37999	0,26614	11,09382	9,374487	32,660756
	101	38,16711	0,20832	8,590132	5,620634	42,180076
	203	44,42561	0,24836	10,03251	7,666640	36,115820
Spin coating on p-type Si	101	38,10701	0,20490	8,450639	5,439572	42,876330
	203	44,37243	0,25862	10,44894	8,316306	34,676461

As can be seen from Table 1, similar micro strain values, dislocation densities and crystal sizes were obtained for the dominant (1 0 1) and (2 0 3) peaks for all samples. Figure 4 shows SEM images of the samples coated by using the SILAR method on (1 1 1) oriented n-type and (1 0 0) oriented p-type Si, respectively. When SEM images are examined, it is seen that the surfaces are completely covered with ZnO.

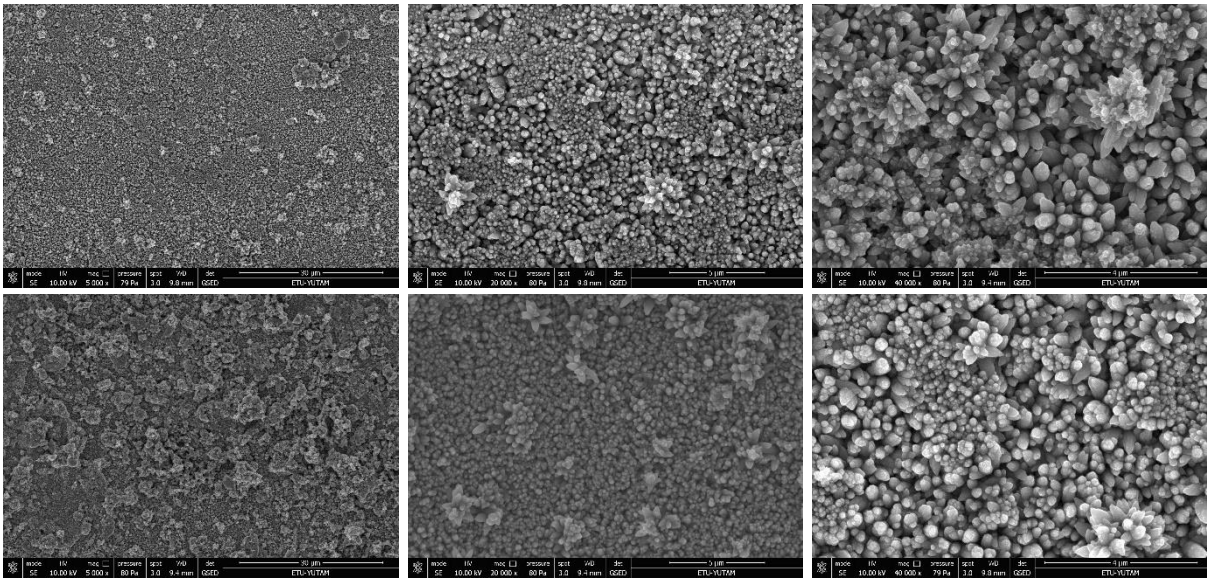

(a) (b) (c)

Figure 4. SEM images of deposited by SILAR method on n-type and p-type Si with (a) 5000x, (b) 20000x, (c) 40000x magnification ratios.

Figure 5 shows SEM images of the samples coated by using the spin coating method on (1 1 1) oriented n-type and (1 0 0) oriented p-type Si, respectively. When the SEM images of the samples are examined, it is seen that the homogeneity of the samples deposited with spin coating is better than the samples deposited with SILAR method. However, difference of the SEM images for SILAR and spin coating deposed samples cannot be explained with XRD data since sizes of the formed crystals are very small compared to the resolution of the obtained SEM images.

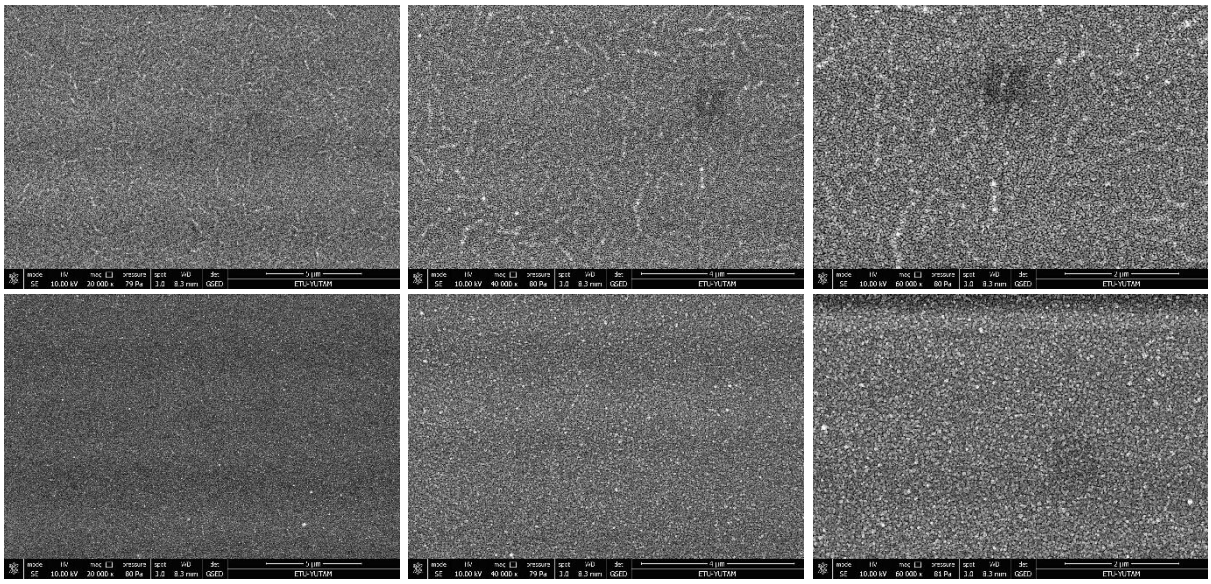

(a) (b) (c)

Figure 5. SEM photos of deposited by spin-coating method on n-type and p-type Si with (a) 20000x, (b) 40000×, (c) 60000× magnification ratios.

Figure 6 shows Tauc plots used to determine band gap of the ZnO thin films deposited by SILAR and spin coating methods. As can be seen from Figure 6, the band gap of the sample deposited by the SILAR method is 3.98 eV and the band gap of the sample deposited by spin coating is 3.88 eV.

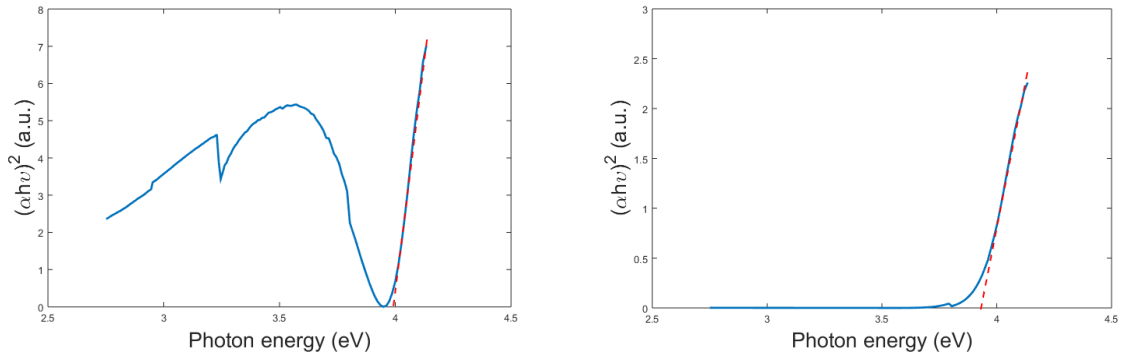

(a) (b)

Figure 6. Tauc plots of the ZnO thin films deposited by (a) SILAR, (b) spin coating method on the n-type Si substrates

Figure 7, 8 and 9 show the photoluminescence spectra graphs under different laser excitation intensities of the samples deposited on n-type, p-type Si by the SILAR method and on n-type Si by the spin-coating method, respectively. The PL system used in the measurements gives at what percent of the maximum power of the excitation laser is operated with, instead of giving exact output power of the laser. Considering that the stimulated emission is dominant due to the nature of the laser and output of the laser is linear in this situation, it is thought that this will not pose any problem in the evaluation of the PL spectrum.

All spectra exhibited similar PL features. Upon examination of the graphs, it was observed that the PL density increased. ZnO thin films luminesce in the visible and UV regions [20]. The emission in the visible region is due to the intrinsic defects of ZnO, and the emission in the UV region is due to excitonic recombination. The peak at approximately 750 nm is more controversial. Some scientists attribute this to defects in the ZnO structure, whereas others have argued that such emission is a quadratic feature of UV emission [21]. In addition, the regions with maximum PL intensity (especially between 500-670 nm) in the graphs draw attention. This was due to the saturation of the detector in the PL system.

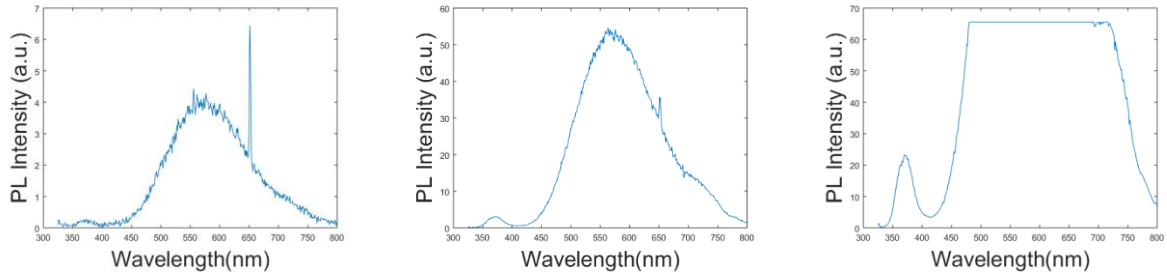

(a) (b) (c)

Figure 7. PL densities of deposited by SILAR method on n-type Si at the laser powers of (a) 0.5%, (b) 1.5%, (c) 7%.

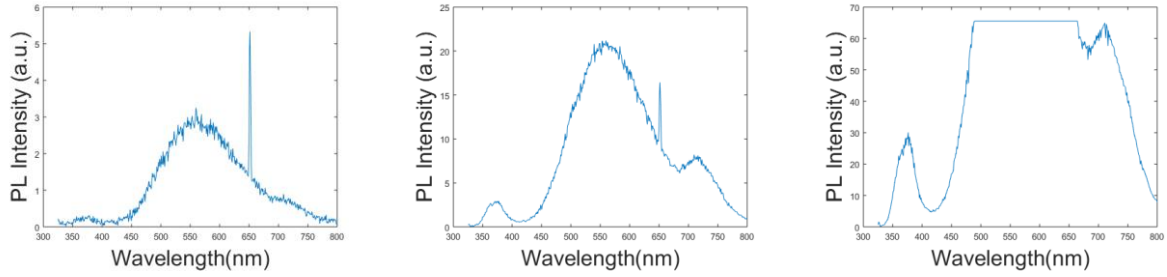

(a) (b) (c)

Figure 8. PL densities of deposited by SILAR method on p-type Si at the laser powers of (a) 0.5%, (b) 1.5%, (c) 7%.

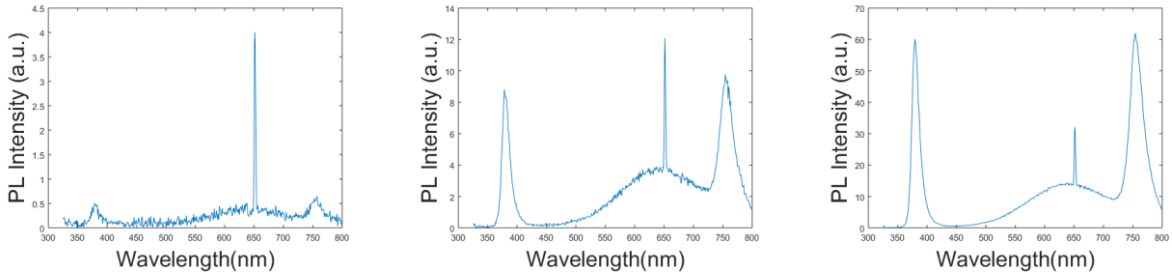

(a) (b) (c)

Figure 9. PL densities of deposited by spin-coating method on n-type Si at the laser powers of (a) 0.5%, (b) 1.5%, (c) 7%.

Figure 10 shows the photoluminescence spectra graphs under different laser excitation intensities of the samples deposited on n-type Si coated by the spincoating method. Notably as the laser intensity increased, the emission intensity in the UV and visible regions also increased.

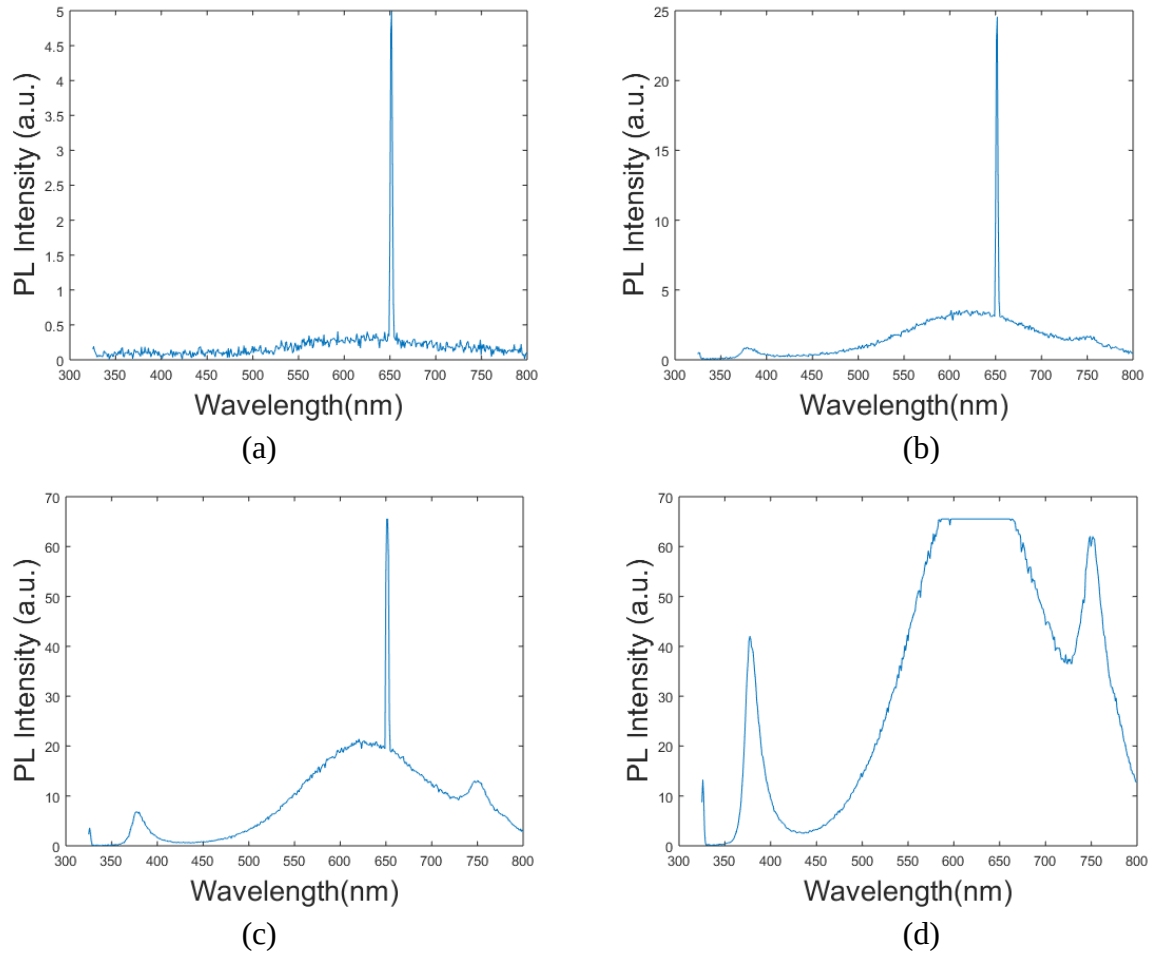

Figure 10. PL densities of deposited by spin-coating method on p-type Si at the laser powers of (a) 0.5%, (b) 1.5%, (c) 7%, (d)15%.

When focusing on PL emissions around 380 nm, it is seen that the samples have the potential for random lasing, given the increased PL emissions due to the increasing excitation intensity. Figure 11 shows the photoluminescence for laser powers of 0.5%, 1.5%, 7% and 15% at 377.25 nm. As mentioned before, higher-power measurements could not be obtained because of the measurement system.

In these measurements, despite the saturation of the detector used in the PL system, an increase in photoluminescence at 377.25 nm was observed. In addition, in the PL figures, the FWHM of the peaks at 377.25 nm decreased with increasing excitation power. These results indicate the well-known random lasing phenomena in ZnO thin films. The direct bandgap nature of ZnO and the random nature of ZnO thin films enable these films to generate high optical gain and high levels of scattering [22]. Owing to these properties, ZnO thin films can exhibit random lasing.

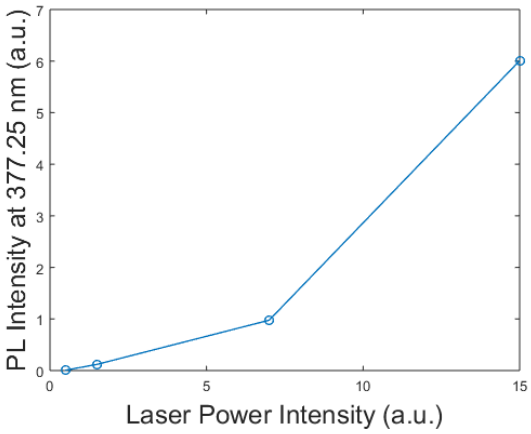

Figure 11. PL densities at 377.25 nm

4. Conclusion

In summary, SILAR and spin-coating methods were used to synthesize ZnO thin films on Si substrates at room temperature. The structural, morphological, and optical properties of the ZnO thin films were investigated. The XRD measurements showed that the ZnO thin films had a polycrystalline structure. The SEM images showed that the surfaces were homogeneously coated. PL measurements showed that the samples gave light output in the UV region, visible region and around 750 nm. When all the measurement results were examined, it was determined that the samples coated using the spin-coating method gave better results than the samples coated using the SILAR method. During the PL measurements, the power could not be increased as desired because the detector in the system was saturated. Despite this problem, PL measurements were performed at four different power levels, and an increase in photoluminescence at 377.25 nm was observed. Moreover, the FWHM of the peaks at 377.25 nm decreased with increasing excitation power. This can indicate well-known random lasing phenomena.

Acknowledgements

This paper is supported by Erzurum Technical University BAP Program (Project No: ETÜ BAP 2017/24).

Ethics in publishing

There are no ethical issues regarding the publication of this study.

Author Contributions

These authors contributed equally to this work.

References

[1] Gupta, T. K. (1990). Application of Zinc Oxide Varistors. *Journal of the American Ceramic Society.* 73(7), 1817–1840.

[2] Raoufi, D. & Raoufi, T. (2009). The effect of heat treatment on the physical properties of sol–gel derived ZnO thin films. *Applied Surface Science,* 255(11), 5812–5817.

[3] Liang, W. Y. & Yoffe, A. D. (1968). Transmission Spectra of ZnO Single Crystals. *Physical Review Letters,* 20(2), 59–62.

[4] Look, D. C. (2001). Recent advances in ZnO materials and devices. *Materials Science and Engineering: B,* 80(1–3), 383–387.

[5] Wan, Q., Li, Q. H., Chen, Y. J., Wang, T. H., He, X. L., Li, J. P. & Lin, C. L. (2004). Fabrication and ethanol sensing characteristics of ZnO nanowire gas sensors. *Applied Physics Letters,* 84(18), 3654.

[6] Barnes, T. M., Leaf, J., Fry, C. & Wolden, C. A. (2005). Room temperature chemical vapor deposition of c-axis ZnO. *Journal of Crystal Growth,* 274(3–4), 412–417.

[7] Water, W. & Chu, S.Y. (2002). Physical and structural properties of ZnO sputtered films. *Materials Letters,* 55(1–2), 67–72.

[8] King, S. L., Gardeniers, J. G. E. & Boyd, I. W. (1996). Pulsed-laser deposited ZnO for device applications. *Applied Surface Science,* 96(98), 811–818.

[9] Ashour, A., Kaid, M. A., El-Sayed, N. Z. & Ibrahim, A. A. (2006). Physical properties of ZnO thin films deposited by spray pyrolysis technique. *Applied Surface Science,* 252(22), 7844–7848.

[10] Liu, Y., Gorla, C. R., Liang, S., Emanetoglu, N., Lu, Y., Shen, H. & Wraback, M. (2000). Ultraviolet detectors based on epitaxial ZnO films grown by MOCVD. *Journal of Electronic Materials*, 29(1), 69–74.

[11] Weng, J., Zhang, Y., Han, G., Zhang, Y., Xu, L., Xu, J., ... & Chen, K. (2005). Electrochemical deposition and characterization of wide band semiconductor ZnO thin film. *Thin Solid Films,* 478(1-2), 25-29.

[12] Yi, S.-H., Choi, S.-K., Jang, J.-M., Kim, J.-A. & Jung, W. G. (2007). Low-temperature growth of ZnO nanorods by chemical bath deposition. *Journal of Colloid and Interface Science*, 313(2), 705–710.

[13] Kaviyarasu, K., Magdalane, C. M., Kanimozhi, K., Kennedy, J., Siddhardha, B., Reddy, E. S., ... & Maaza, M. (2017). Elucidation of photocatalysis, photoluminescence and antibacterial studies of ZnO thin films by spin coating method. *Journal of Photochemistry and Photobiology B: Biology,* 173, 466-475.

[14] Lanjewar, M. & Gohel, J. V. (2017). Enhanced performance of Ag-doped ZnO and pure ZnO thin films DSSCs prepared by sol-gel spin coating. *Inorganic and Nano-Metal Chemistry,* 47(7), 1090–1096.

[15] Youl Bae, H. & Man Choi, G. (1999). Electrical and reducing gas sensing properties of ZnO and ZnO–CuO thin films fabricated by spin coating method. *Sensors and Actuators B: Chemical,* 55(1), 47–54.

[16] Kumar, P. S., Raj, A. D., Mangalaraj, D. & Nataraj, D. (2010). Hydrophobic ZnO nanostructured thin films on glass substrate by simple successive ionic layer absorption and reaction (SILAR) method. *Thin Solid Films, Symposium on Functional Ceramic*

Materials, Oxide Thin Films and Heterostructures (ICMAT 2009), 518(24, Supplement), e183–e186.

[17] Pathan, H. M. & Lokhande, C. D. (2004). Deposition of metal chalcogenide thin films by successive ionic layer adsorption and reaction (SILAR) method. *Bulletin of Materials Science*, 27(2), 85–111.

[18] Shei, S. C. & Lee, P. Y. (2013). Influence of rinsing temperature on properties of ZnO thin films prepared by SILAR method with propylene glycol. *Journal of Alloys and Compounds*, 546, 165–170.

[19] Gür, E., Asıl, H., Coşkun, C., Tüzemen, S., Meral, K., Onganer, Y. & Şerifoğlu, K. (2008). Optical and structural properties of ZnO thin films; effects of high energy electron irradiation and annealing. *Nuclear Instruments and Methods in Physics Research Section B: Beam Interactions with Materials and Atoms*. 266(9), 2021–2026.

[20] Rauwel, P., Salumaa, M., Aasna, A., Galeckas, A. & Rauwel, E. (2016). A Review of the Synthesis and Photoluminescence Properties of Hybrid ZnO and Carbon Nanomaterials. *Journal of Nanomaterials*, 2016, e5320625.

[21] Guidelli, E. J., Baffa, O. & Clarke, D. R. (2015). Enhanced UV Emission From Silver/ZnO And Gold/ZnO Core-Shell Nanoparticles: Photoluminescence, Radioluminescence, And Optically Stimulated Luminescence. *Scientific Reports.* 5(1), 14004.

[22] Fallert, J., Dietz, R. J. B., Hauser, M., Stelzl, F., Klingshirn, C. & Kalt, H. (2009). Random lasing in ZnO nanocrystals. *Journal of Luminescence, Special Issue based on The 15th International Conference on Luminescence and Optical Spectroscopy of Condensed Matter (ICL'08),* 129(12), 1685–1688.